Jurnal Ekologi, Masyarakat dan Sains
E-ISSN: 2720-9717
Volume 6, Nomor 2, 2025
ECOTAS
https://journals.ecotas.org/index.php/ems
https://doi.org/10.55448/ems

Artikel

Application of the SVD Method Using Magnetic Data to Identify Subsurface Structures in the Geothermal Area of Sonai Village and its Surrounding regions, Puriala, Konawe

Wa Ode Salmatia[1], *Abdul* Manan[1], Bahdad[2], *Rani* Chahyani[3], and *La Ode* Andimbara[1]

[1]Department of Geophysical Engineering, Universitas Halu Oleo, Kampus Hijau Bumi Tridharma Anduonohu, Kota Kendari, Indonesia
[2]Department of Oceanography, Universitas Halu Oleo, Kampus Hijau Bumi Tridharma Anduonohu, Kota Kendari, Indonesia
[3]Study Program of Physics Education, Institut Agama Islam Negeri (IAIN) Kendari, Jln. Sultan Qaimuddin No. 17, Kota Kendari, Indonesia
Corresponding Author: amanan@uho.ac.id

Riwayat Artikel:

Masuk: 04-06-2025
Diterima: 19-09-2025
Dipublikasi: 01-01-2026

Cara Mengutip
Salmatia, Wa Ode, Abdul Manan, Bahdad, Rani Chahyani, dan La Ode Andimbara. 2026. "Application of SVD Method Using Magnetic Data to Identify Subsurface Structures at the Geothermal Area of Sonai Village and Its Surroundings, Puriala, Konawe". Jurnal Ekologi, Masyarakat Dan Sains 6 (2): 215-24. https://doi.org/10.55448/ayq9y305.

Abstract: The subsurface structure in the Sonai geothermal area and its surrounding regions has not been clearly identified, thus necessitating the implementation of this research. The research was conducted using the Second Vertical Derivative (SVD) method for magnetic data. The data used were obtained through measurements at 126 points. The total magnetic anomaly values measured after applying Diurnal and IGRF corrections ranged from approximately -171.17 to 82.47 nT. After performing Upward Continuation and further processing, the residual magnetic field anomaly values ranged from approximately -150 to 90 nT. Then the SVD method is applied to residual anomalous data that has been reduced to the Pole. Based on the SVD method and 2D modeling, several types of fault structures were identified in the research area, comprising two reverse/thrust faults and four normal faults. The nearest minor fault to the hot spring manifestation is located at a distance of approximately 16 meters. These minor faults are considered geothermal conduits that cause the heating of water in the manifestation area. Furthermore, it was identified that the subsurface layers of the Sonai area and its surrounding regions consist of three formations, which are the Alluvium Deposits, the Alangga Formation, and the Ultramafic Complex. Understanding the structure and formation of rocks can enhance the comprehension of the causes of hot spring in an area.

Keywords: Geothermal, magnetic anomaly, subsurface structure, SVD method, 2D modeling

1 INTRODUCTION

Indonesia is among the countries with significant geothermal resource potential. Geothermal energy is a natural resource in the form of hot water or steam generated within subsurface reservoirs through heating processes around volcanic regions or via non-volcanic mechanisms (Mahardhika et al., 2020). One of the regions in Indonesia that possesses geothermal potential is Southeast Sulawesi.

The geothermal system in the southeastern part of Sulawesi is a non-volcanic system (Anonymous, 2017) caused by a combination of the influence of geological structure patterns and residual heat from magmatic activity that appears in metamorphic and sedimentary rock environments (Jailani, 2015). Non-volcanic systems are usually associated with the presence of faults in the Earth's subsurface (Risdianto et al., 2015).

Heat transfer in geothermal systems occurs in the upper mantle and crust, and proceeds from the heat source to the heat release site on the surface. In addition to the existence of geological structures such as faults, the controllers in geothermal systems include heat sources, reservoir rocks, and water catchment areas (Suryadi et al., 2017).

In Southeast Sulawesi, there is a geothermal manifestation area in Sonai Village and its surrounding regions. This area was studied by the Geological Agency of the Ministry of Energy and Mineral Resources RI in 2015 by conducting a geochemical survey (Anonymous, 2017). Meanwhile, the distribution of hot fluids in this area was studied by Baskara (2020) using the Wenner-Schlumberger configuration resistivity method. Hot spring in the Sonai area and its surrounding regions are estimated to appear through fractures in ultrabasic rocks. Most recently, Ratu et al. (2025) has also studied this geothermal area using the Pseudo-Gravity method.

Geologically, in Puriala District there is a Konaweha fault that cuts Alluvial Deposits in the Wawotobi plain and cuts rocks along the Konaweha River which indicates that this fault is still active until now (Zakaria and Sidarto, 2015). The vibration activity of this fault is thought to cause minor faults around it. Fault is one of the geological structures that plays an important role in the geothermal system because it can be a path for hot fluids to reach the surface. Therefore, identifying the presence and knowing the types of minor faults in the subsurface is very important in geothermal exploration.

One method that can be used to estimate the subsurface structures, especially to determine the presence of minor faults, is the magnetic method. In addition, this method can also be used to determine other geological structures such as folds and igneous intrusions (Ngoh et al., 2017). This method measures the intensity of the magnetic field on the surface caused by variations in susceptibility or geological structures in the Earth's subsurface (Medhus and Klinkby, 2023).

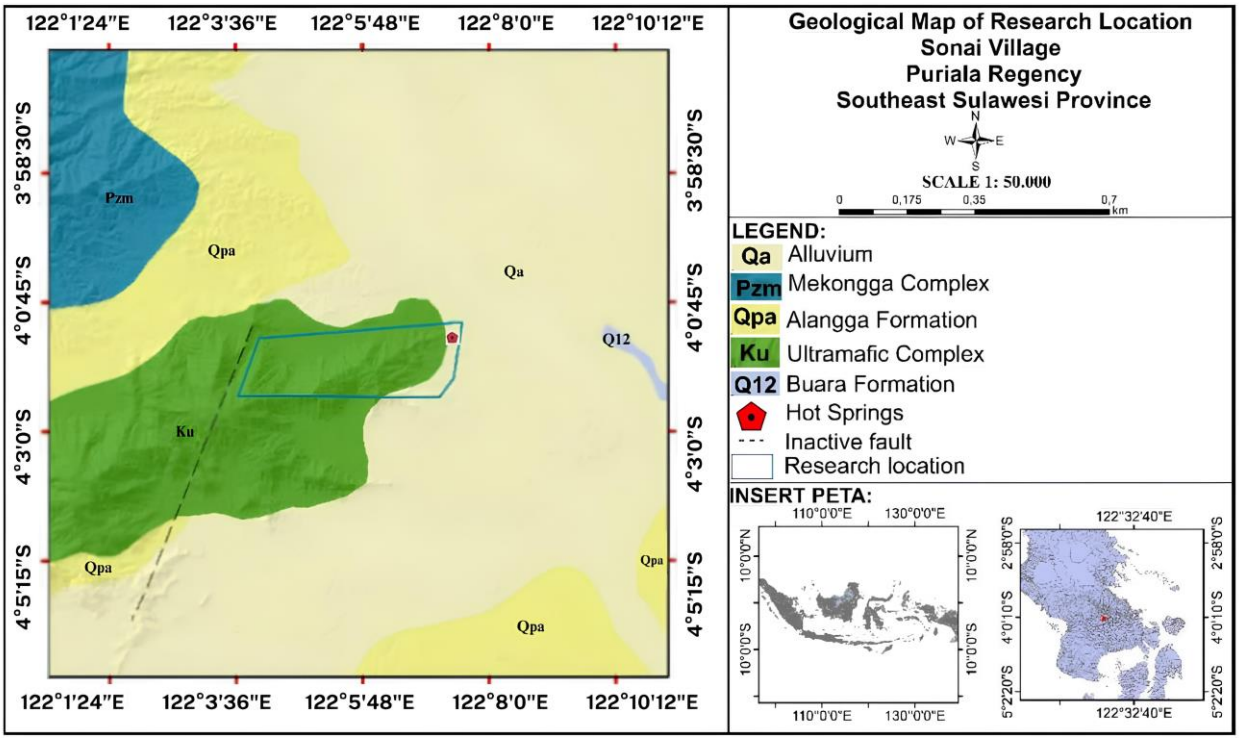

Figure 1. Regional geological map of the research area (Sariani et al., 2024)

This research was conducted to identify the subsurface structure, particularly the existence and types of minor faults in the Sonai geothermal area and its surrounding regions, as well as the rock formations that compose the area. To find out the type of minor faults in the subsurface of the Sonai area and its surrounding regions, the Second Vertical Derivative (SVD) method can be used. The method is a relatively simple approach for determining the types within an area. The type of faults is known based on the comparison of the maximum and minimum absolute values of SVD. In Hofi et al. (2024) and Mirnanda et al. (2022) it is stated that this method can describe the residual anomaly values associated with shallow structures. Understanding the structural features

and formation of rocks can enhance insight into the causes of hot spring occurrences in the research area.

2 RESEARCH METHOD

2.1 Regional Geology of Puriala Area

Regionally, Puriala District is included in the geological map of the Kolaka Sheet (Simandjuntak et al., 1993). Based on the rock assemblage and its characteristics, the geology of the Kolaka Sheet can be divided into two geological belts, which are the Tinodo Belt and the Hialu Belt. The rocks found in the Tinodo Belt which are the basement rocks are Paleozoic Metamorphic rocks (Pzm) and are thought to be Carboniferous in age, consisting of mica schist, quartz schist, chlorite schist, graphite mica schist, slate and gneiss. The rocks found in the Hialu Belt are Ophiolite Rocks (Ku). The Ophiolite Complex rocks are part of the East Sulawesi Ophiolite zone which consists of ultramafic and mafic rocks and deep-sea sediments (pelagic sediments). This complex is widespread in Southeast Sulawesi from the eastern tip of the East Arm to the Southeast Arm of Sulawesi. This complex is estimated to be of Lower Cretaceous age consisting of peridotite, dunite, harzburgite, lhersolite, and pyroxenite rocks. The youngest rocks in this sheet are Alluvium (Qa) consisting of river, swamp and beach deposits (Zakaria and Sidarto, 2015).

Based on Figure 1, the research area is still influenced by the Konaweha fault which is trending Northwest-Southeast. The formations found in this area are Alluvium Deposits, Alangga Formation and Ultramafic Complex.

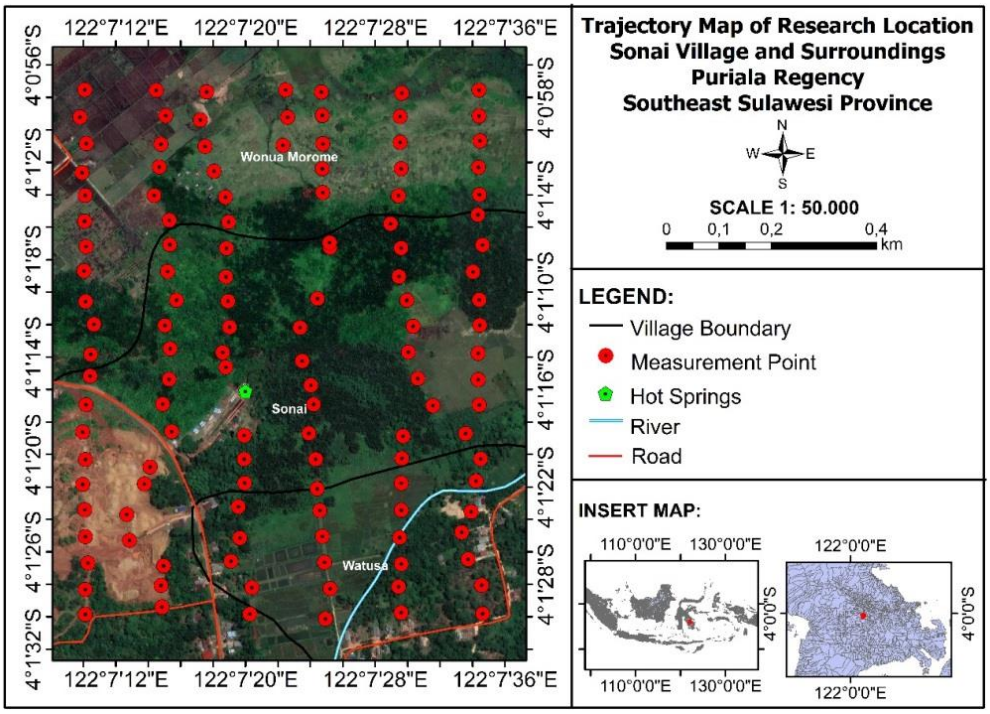

Figure 2. Map of measurement points

2.2 Location and Research Data

The research location is administratively located in Sonai Village, and partly in Watusa village and Wonua Morome village, Puriala District, Konawe Regency, Southeast Sulawesi Province. The research data uses total magnetic field data obtained from the measurement results of 1 set of Proton Magnetometer and Gradiometer (PMG-2) instruments.

Total magnetic field measurements were conducted on November 12-13, 2023 at 126 points in 6 trajectories and an area in a grid of ±1,050 m x 900 m. Each point was measured 4 times with a N180^{o}S trajectory direction as in Figure 2. In addition, magnetic inclination and declination angle data from the research location were also used, obtained from the IAGA website, www.ngdc.noaa.gov/.

2.3 Data Processing

Data processing in this research was conducted in several stages. These stages are further explained in the description below:

1. *Calculating the Total Magnetic Field value of each measurement point*

The single total magnetic field value measured by the PMG-2 instrumet is calculated using the Moving Average (MA) formula:

$$y[i] = \sum_{j=0}^{M-1} x[1+j] \quad (1)$$

where $x[1+j]$ is the input signal value, $y[i]$ is the output signal, and M is the average value of the input values.

2. *Performing Diurnal Correction*
Diurnal correction is a data normalization to eliminate daily magnetic fluctuations. Correction is done using the formula (Sariani et al., 2024; Pancasari et al., 2020; Fikar et al., 2019):

$$\Delta H_d = \left(\frac{t_n - t_{in}}{t_{en} - t_{in}} \right) \left(H_{en} - H_{in} \right) \quad (2)$$

where ΔH_d is the diurnal correction, H_{en} is the magnetic field value at the end point, H_{in} is the magnetic field value at the starting point, t_{in} is the measurement time at the starting point, t_{en} is the measurement time at the end point, and t_n is the measurement at point n.

3. *Performing IGRF Correction*
IGRF (International Geomagnetic Reference Field) correction is a correction made to eliminate the influence of the Earth's main magnetic field. The IGRF value of the research area was obtained through the IAGA (The International Association of Geomagnetism and Aeronomy) website, which is www.ngdc.noaa.gov/. IGRF correction is calculated using the formula (Pancasari et al., 2020; Fikar et al., 2019):

$$\Delta H_t = H_h \pm \Delta H_d - H_o \quad (3)$$

where ΔH_t is the total magnetic anomaly, H_h is the H value at each measurement point, ΔH_d is the diurnal correction, and H_o is the IGRF correction for the geothermal area of Sonai village and its surroundings.

4. *Performing Upward Continuation*
Continuation serves to separate regional magnetic field anomalies from total magnetic field anomalies (Kamureyina et al., 2019). Upward Continuation ($\Delta H_{continuation}$) is performed after the total magnetic field data is corrected for diurnal variation and IGRF.

5. *Residual Magnetic Field Anomaly*
The target of the research is residual (local) anomalies. To obtain residual anomalies, follow the formula (Pancasari et al., 2020):

$$\Delta H_r = \Delta H_t - \Delta H_{continuation} \quad (4)$$

where ΔH_r is the residual magnetic field anomaly, ΔH_t is the total magnetic anomaly and $\Delta H_{continuation}$ is the magnetic anomaly resulting from Upward Continuation.

6. *Performing Reduction to the Pole*
Reduction to Pole (RTP) transformation is performed to transform the residual magnetic field anomaly to polar coordinates. It makes the magnetic field anomaly located directly above the object causing the anomaly (monopole anomaly) (Sehah et al., 2023).

7. *Applying the Second Vertical Derivative (SVD) Method*
The Second Vertical Derivative (SVD) method is applied to residual magnetic field anomaly data that has been reduced to the pole. The Second Vertical Derivative (SVD) method is a second order derivative of the Horizontal Gradient (HG) filter which acts as a high pass filter. The general equation of the SVD method is (Hofi et al., 2024; Mirnanda et al., 2022):

$$\frac{\partial^2 \Delta H}{\partial z^2} = -\left(\frac{\partial^2 \Delta H}{\partial x^2} + \frac{\partial^2 \Delta H}{\partial y^2} \right) \quad (5)$$

The types of faults can be identified from the maximum and minimum SVD values based on the criteria (Maulidah et al., 2022; Widodo et al., 2016):
- $|SVD|_{max} > |SVD|_{min}$: normal/downward fault,
- $|SVD|_{max} < |SVD|_{min}$: thrust/reverse fault,
- $|SVD|_{max} = |SVD|_{min}$: strike-slip fault.

8. *Performing 2D Modeling*
2D modeling is based on the results of slicing the residual magnetic anomaly map that has been reduced to the Pole. The slices for 2D modeling correspond to the slices on the SVD map. The estimation of the presence of minor faults in the subsurface is based on the results of applying the Second Vertical Derivative (SVD) method. While this modeling is carried out to see the 2D cross-section of the subsurface layer in the research area, especially the existence of minor faults in 2D. To determine the types of rocks (layers) in this study, refer to the table in the book by Telford et al. (1990). The table shows the susceptibility values of several minerals and rocks.

3 RESULTS AND DISCUSSION

3.1 Total Magnetic Field Measurement Results

Magnetic field measurements were conducted in the geothermal area of Sonai village and its surrounding regions which are geographically located at the base station

4°1'14.63"S and 122°7'18.8"E using 1 set of PMG-2 instrument in the N180ºS direction. The total magnetic field value obtained was 42,220.6 nT to 42,469.2 nT as shown in Figure 3.

Figure 3 shows the various contour closures, some are tighter and some are looser. The variety of closures is caused by the distribution of magnetic susceptibility of rocks in the subsurface which is not homogeneous. In addition, it is also thought to be caused by the presence of geological structures such as faults in the subsurface.

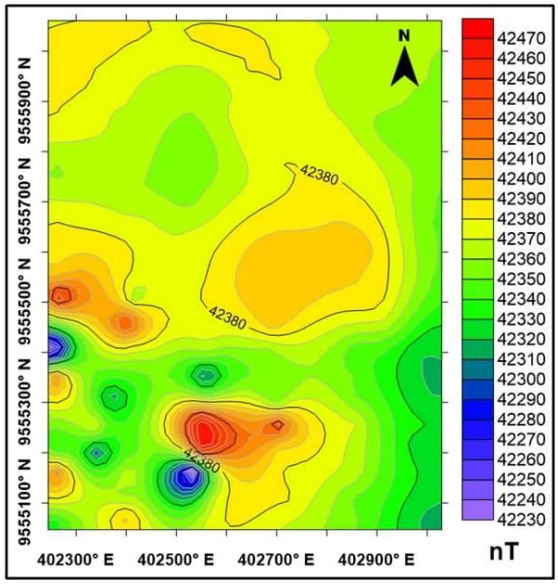

Figure 3. Contour of the total magnetic field resulting from the measurement

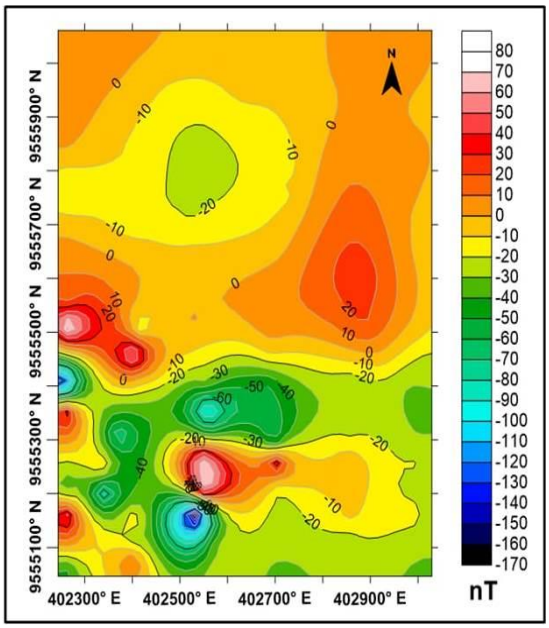

Figure 4. Corrected total magnetic field anomaly contour

3.2 Total Magnetic Field Anomaly

The total magnetic field anomaly values that have undergone diurnal and IGRF corrections show an anomaly distribution pattern in the research area with varying intensities of around -171.2 nT to 82.5 nT as in Figure 4. The contours in this figure show that there is still the influence of residual and regional anomalies on the total magnetic field contour pattern. Diurnal and IGRF corrections are performed using equations (2) and (3).

3.3 Upward Continuation Transformation

Upward Continuation transformation was performed 4 times, which are at heights of 150 meters, 200 meters, 250 meters and 300 meters as in Figure 5. The results of the continuation process show changes in the anomaly contour that have stabilized at a height of 300 meters, which indicates the appearance of regional anomalies and the increasingly reduced residual anomalies.

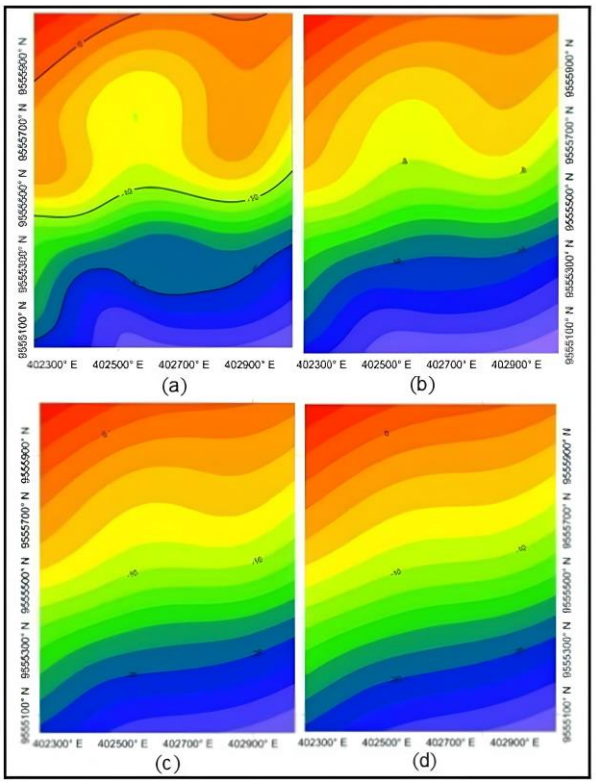

Figure 5. Upward Continuation contours at heights of (a). 150 m, (b). 200 m, (c). 250 m, and (d). 300 m

3.4 Residual Magnetic Field Anomaly

To obtain the residual anomaly that is the target of the research, further processing is performed after the Upward Continuation process. The residual anomaly follows equation (4), and the result is Figure 6.

Figure 6 shows magnetic contour with varying intensities of around -150 to 90 nT. The magnetic intensity that tends to be high is located mostly in the West-Northeast, a small part is located in the South and West. While the dominant low magnetic intensity is located mostly in the Southwest-South, North-Northwest directions and a small part is located in the South, Southwest-East directions.

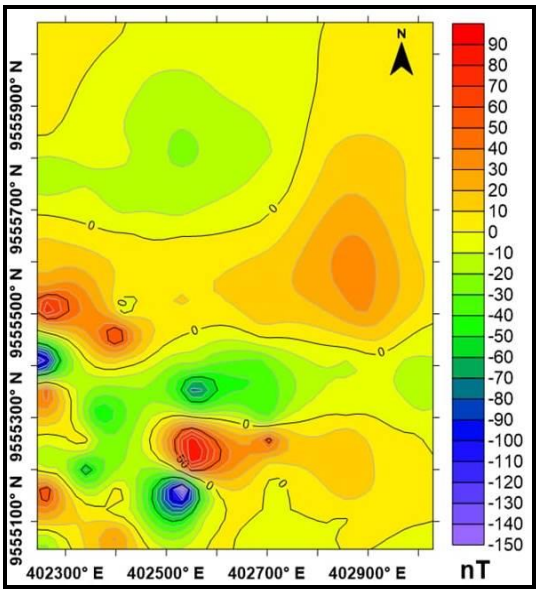

Figure 6. Contour of residual magnetic field anomaly

3.5 RTP Transformation

On the residual anomaly data, a Reduction to Pole (RTP) transformation was performed to eliminate the influence of the magnetic inclination angle at the research location. The transformation result in Figure 7 shows a very significant difference in anomaly closures when compared to the closures before the transformation.

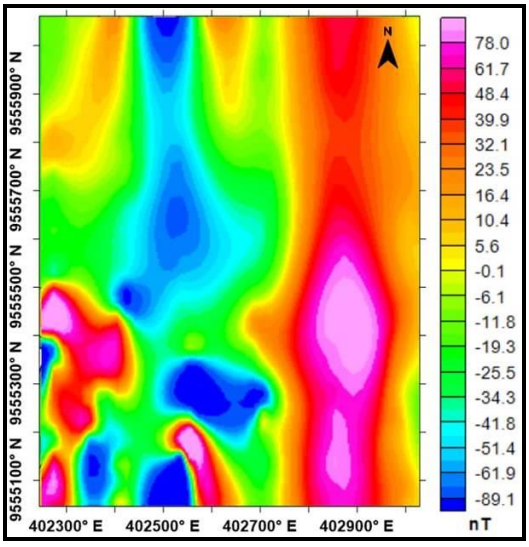

Figure 7. Residual magnetic anomaly contour after RTP process

3.6. Application of the Second Vertical Derivative (SVD) Method

The residual magnetic field anomaly that has been processed with RTP, then the Second Vertical Derivative (SVD) method is applied to it. On the SVD map, 2 slices are made, which are slices A-A' and B-B' to determine the types of minor faults in the research area as in Figure 8.

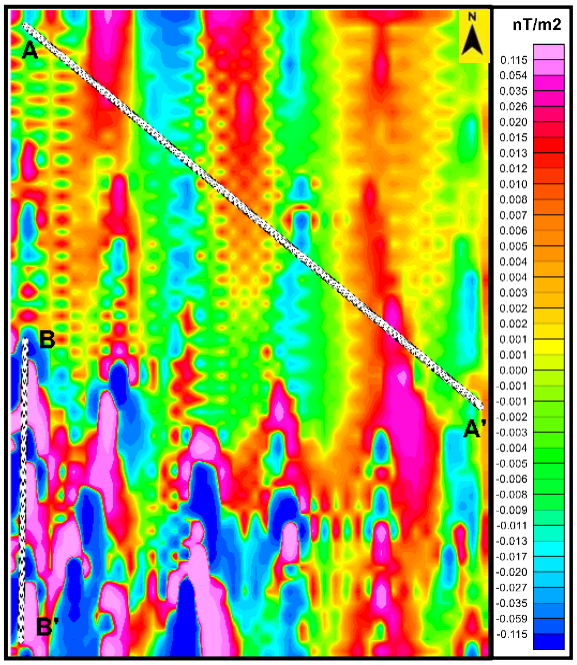

Figure 8. Direction of A-A' and B-B' slices on the local anomaly map resulting from SVD

The result of the A-A' slice in Figure 8 with a length of approximately 1,039 meters show the presence of 5 minor fault structures in the subsurface based on the minimum and maximum SVD values which can be seen in Figure 9, which are at points A, B, C, D and E.

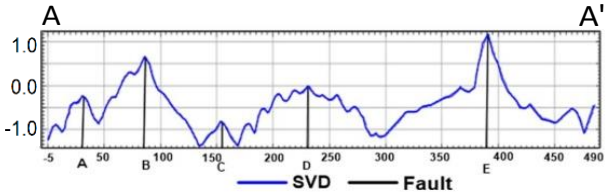

Figure 9. Digitization result of A-A' slice

In Figure 9, point A has a maximum value of 0.007 nT/m^2 with a minimum value of -0.014 nT/m^2, so the minor fault at this location is thought to be a reverse/thrust because the maximum SVD value is smaller than the minimum SVD value. For point B, the maximum

value is 0.023 nT/m^2 and the minimum value is -0.017 nT/m^2, so it is thought to be a normal fault location because the maximum SVD value is greater than the minimum SVD value. For point C, the maximum SVD value is 0.010 nT/m^2 and the minimum SVD value is -0.017 nT/m^2 so it is thought to be a reverse/thrust fault location. For point D, the maximum SVD value is 0.034 nT/m^2 and the minimum SVD value is -0.013 nT/m^2 as a normal fault, likewise for point E is a normal fault because it has a maximum SVD value of 0.031 nT/m^2 and a minimum SVD of -0.011 nT/m^2.

The fault at point D is located close to the geothermal manifestation location of Sonai village and its surrounding regions, which is about 16 meters away, so it is thought that the emergence of geothermal manifestations at this location is partly due to the presence of a normal/downward fault structure which is a medium for fluid flow out to the surface. This fault is located at coordinates 4°1'16.41" South Latitude and 122°7'23.23" East Longitude.

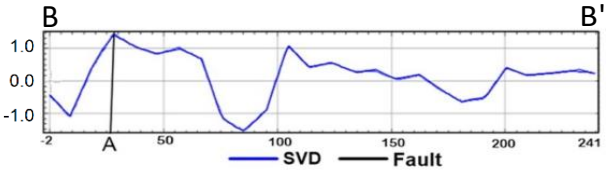

Figure 10. Digitization result of B-B' slice

For the B-B' slice in Figure 8, it extends ±443.21 meters. The digitization results of the B-B' slice can be seen in Figure 10 which only shows the presence of one fault at point A. The fault at point A is thought to be a normal fault because its maximum SVD value is greater than its minimum SVD value where at point A it has a maximum absolute SVD value of 0.293 nT/m^2 with a minimum SVD value of -0.215 nT/m^2.

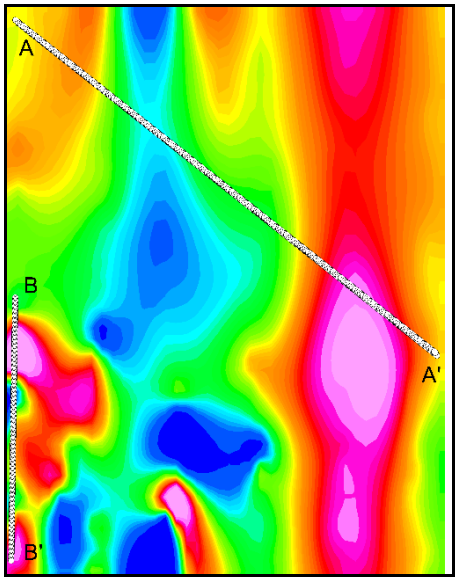

Figure 11. Directions of A-A' and B-B' slices on the residual anomaly map that has been RTP

3.7 2D Modeling Results and Subsurface Structure

2D modeling is done to see the 2D cross-section in the research location. The slices for 2D modeling are done on the residual anomaly map that has been reduced to the Pole (RTP), and can be seen in Figure 11. There are 2 slices, which are slices A-A' and B-B' which correspond to the slices on the SVD map in Figure 8. The results of 2D modeling for A-A' and B-B' slices can be seen in Figures 12 and 13, respectively.

2D modeling for the A-A' slice in Figure 12 crosses from Northwest to East of the research area. The results of 2D modeling show that the research area consists of 3 layers. For the first layer, there are rocks with a magnetic susceptibility of 0.03501 cgs which are sandstone, susceptibility of 0.000001 cgs is sand and magnetic susceptibility of 0.002150 cgs is clay from Alluvium Deposits. In the second layer, there is only a magnetic susceptibility of 0.00545 cgs which is a conglomerate from the Alangga Formation, likewise the third layer only has a magnetic susceptibility of 0.01 cgs which is a peridotite from the Ultramafic Complex. The modeling also shows the presence of 5 minor fault structures marked with black lines and labeled F_A, F_B, F_C, F_D and F_E, which based on the results of the SVD map analysis in Figure 9 are 2 reverse/thrust faults and 3 normal faults.

Figure 13 shows the results of 2D modeling for the B-B' slice that crosses from North to South of the research area. In this 2D model, there are also 3 layers in the research area. For the first layer, it consists of rocks with a magnetic susceptibility of 0.0040 cgs which is sandstone, a susceptibility of 0.000001 cgs is sand and a susceptibility of 0.002251 cgs which is clay from Alluvium Deposits. For the second layer, it only consists of rocks with a magnetic susceptibility value of 0.004501 cgs which is conglomerate from the Alangga Formation, likewise the third layer only consists of rocks with a magnetic susceptibility value of 0.01 cgs which is peridotite from the Ultramafic Complex. The modeling also shows the presence of 1 fault marked with a black line and labeled F_F, and based on the results of the SVD map analysis in Figure 10, it is a normal fault.

Peridotite from the Ultramafic Complex in the third layer in the subsurface of the research area function as impermeable rocks so that subsurface fluids do not rise to the surface. While

the existence of faults that control heat sources (fluids or steam) to (near) the surface.

In Tamburaka (2019) it is stated that the research area is regionally influenced by the Konaweha shear-fault. As a result of the movement of the shear fault, minor faults have emerged which are the cause of the emergence of geothermal manifestation in the research area. This shows that the type of geothermal in Sonai Village and surrounding regions is non-volcanic geothermal.

The findings of this research are consistent with those reported by Ratu et al. (2025) and Sariani et al. (2024), who conducted research in the same area but using different methods. Ratu et al. (2025) employed the Pseudo-Gravity method, while Sariani et al. (2024) utilized the Euler-Deconvolution method. Both studies indicate that the geothermal system in the Sonai geothermal area and surrounding regions is controlled by several minor faults. Furthermore, it was identified that the geothermal region is composed of multiple rock formations, specifically the Alluvium Deposits, Alangga Formation and Ultramafic Complex.

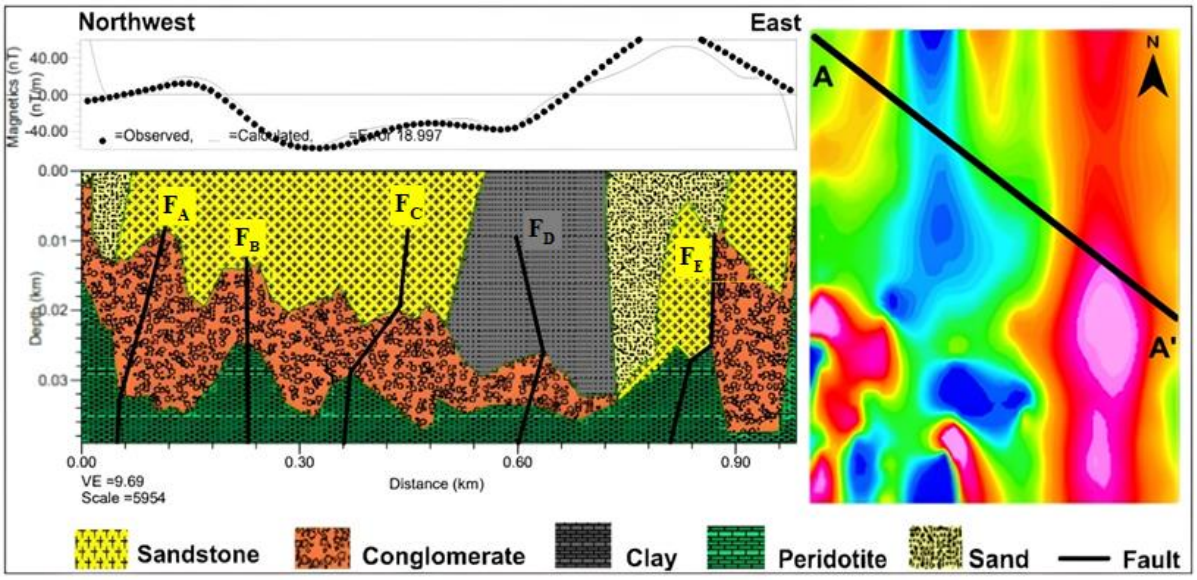

Figure 12. 2D cross-section of A-A' slice

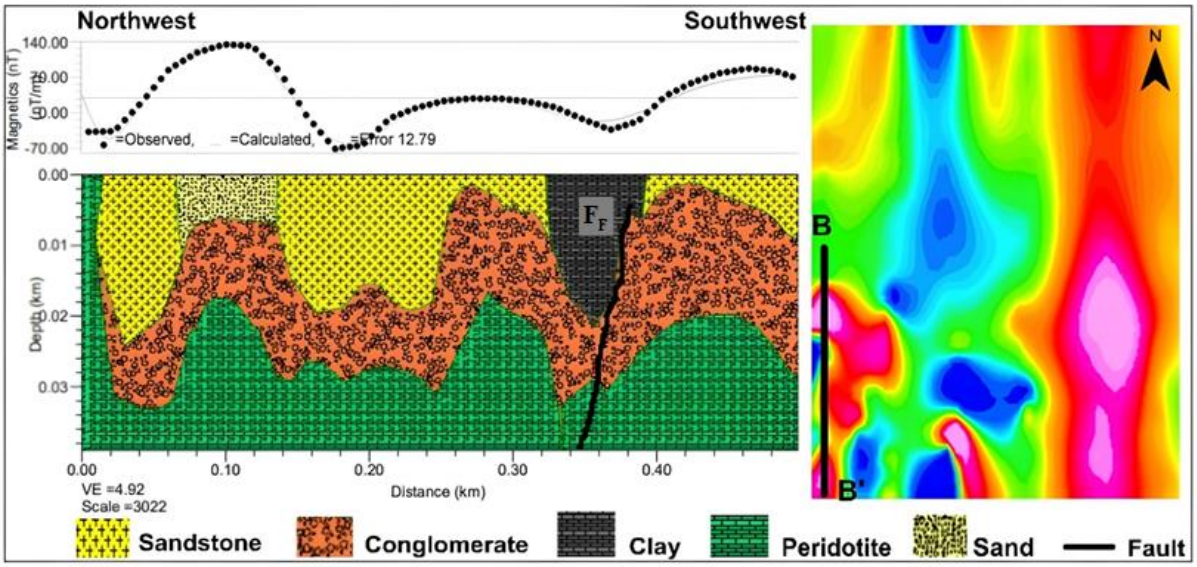

Figure 13. 2D cross-section of B-B' slice

4 CONCLUSION

Based on the research results, it can be concluded that in the Sonai area and its surrounding regions there are several minor faults consisting of normal faults and reverse/thrust faults. The type of reverse/thrust fault is found at

2 points and normal faults at 4 points. The closest fault to the manifestation is at coordinates 4°1'16.41"S and 122°7'23.23"E which is ±16 meters away. These minor faults are thought to be the source of heat (fluid or steam) to come out to the surface. In addition, it is also known that the research area is composed of 3 formations, which are Alluvium Deposits, Alangga Formation and Ultramafic Complex. To achieve more reliable and comprehensive results, further investigations should incorporate additional geophysical methods, such as the gravity method.

REFERENCES

Anonymous. (2017). *Potensi Panas Bumi Indonesia Jilid 1*. Jakarta: Badan Geologi, Kementerian ESDM.

Baskara, M.Y. (2020). *Identifikasi Sebaran Fluida Panas Daerah Panasbumi Puriala, Kabupaten Konawe Menggunakan Metode Geolistrik Resistivitas Konfigurasi Wenner-Schlumberger*. Skripsi. Kendari: Universitas Halu Oleo.

Fikar, M., Hamimu, L., Manan, A. & Suyanto, I. (2019). Pemodelan 2D Data Magnetik Menggunakan Transformasi RTP untuk Pendugaan Sesar di Daerah Kasihan, Pacitan, Jawa Timur. *Jurnal Rekayasa Geofisika Indonesia (JRGI)*, 02(01), 33-42. https://ojs.uho.ac.id/index.php/jrgi/article/view/8721

Hofi, L.N., Maryanto, S., Susilo, A., Andinisari, R. & Wuryani, S.D. (2024). Fault Detection and Subsurface Model Based on Gravity Data in Pronojiwo, Lumajang, Indonesia. *EVERGREEN Joint Journal of Novel Carbon Resource Sciences & Green Asia Strategy*, 11(3), 1666-1675. https://doi.org/10.5109/7236820

Jailani, M. (2015). *Analisis Geologi dan Geokimia untuk Menentukan Keprospekan Sistem Panas Bumi Non-Vulkanik Daerah Amoholo-Sumbersari dan Sekitarnya Kecamatan Moramo, Kabupaten Konawe Selatan, Provinsi Sulawesi Tenggara*. Tesis. Yogyakarta: UPN Veteran Yogyakarta. http://eprints.upnyk.ac.id/id/eprint/1577

Kamureyina, E., Omang, B.O., Simon, K., Owolabi, A., & Nur, A. (2019). Determination of Hydrocarbon Potentials Using High Resolution Aeromagnetic Data over Sokoto Basin Northwestern Nigeria. *International Journal of Geosciences*, *10*(*04*), 419-438. https://doi.org/10.4236/ijg.2019.104024

Mahardhika, R, Said, Y.M., Resta, I.L., & Mastur, A.K. (2020). Identifikasi Keberadaan Manifestasi Daerah Panasbumi Gunung Sumbing Jangkat Berdasarkan Interpretasi Data Landsat 8 dan Geolistrik, *Jurnal Geologi dan Sumberdaya Mineral*, 21(4), 207-215. https://doi.org/10.33332/jgsm.geologi.v21i4.486

Maulidah, H., Pratowo, T., & Realita, A. (2022). Identifikasi Sesar Grindulu dengan Memanfaatkan Metode Gravitasi. *Inovasi Fisika Indonesia* (IFI), 11(2), 20-27. https://doi.org/10.26740/ifi.v11n02.p20-27

Medhus, A.B., & Klinkby, L. (2023). *Engineering Geophysics 1st Edition*. Leiden: CRC Press/Balkema.

Mirnanda, E., Simatupang, V.S., & Prabowo, H. (2022). Geological Interpretation of 2D Gravity Modeling in Tulung Selapan Area and Surroundings, South Sumatera Basin. *Bulletin of the Marine Geology*, 37(2), 107-119. http://dx.doi.org/10.32693/bomg.37.2.2022.796

Ngoh, J.N., Mbarga, T.N., Assembe, S.P., Meying, A., Owono, O.U., & Tabod, T.C. (2017). Evidence of Structural Facts Inferred from Aeromagnetic Data Analysis over the Guider-Maroua Area (Northern Cameroon). *International Journal of Geosciences (IJG)*, *8*(*6*), 781-800. https://doi.org/10.4236/ijg.2017.86044

Pancasari, A., Safani, J., & Manan, A. (2020). Interpretasi Struktur Bawah Permukaan Daerah Kota Kendari Berdasarkan Data Anomali Medan Magnetik Lokal. *Jurnal Rekayasa Geofisika Indonesia (JRGI)*, 02(02), 45-53. https://ojs.uho.ac.id/index.php/jrgi/article/view/15211

Ratu, M.D., Manan, A., Bahdad, Chahyani, R. (2025). Identification of Subsurface Structure Using the Pseudo-Gravity Method of Magnetic Data at the Geothermal Area of Sonai Village and its Surroundings, Puriala, Konawe Regency. *Indonesian Physics Communication*, 22(2), 73-84. http://dx.doi.org/10.31258/jkfi.22.2.73-84

Risdianto, D., Permana, A., Wibowo, A., Sugianto, A., & Hermawan, D. (2015). *Sistem Panasbumi Non-Vulkanik di Sulawesi*. Bandung: Badan Geologi, Kementerian ESDM.

Sariani, Manan, A., Bahdad, & Chahyani, R. (2024). Estimation of Subsurface Structure Using Euler Deconvolution Method of

Magnetic Data at the Geothermal Area of Sonai Village and its Surroundings, Konawe Regency. *JURNAL GEOCELEBES*, *8*(*2*), 162-177. https://doi.org/10.70561/geocelebes.v8i2.36380

Sehah, Prabowo, U.N., Raharjo, S.A., & Prasetya, R.I. (2023). Two-Dimensional Modeling of Magnetic Anomaly Data Reduced to the Poles in the Andesitic Prospect Area of the Southeast Slope of Slamet Volcano, Indonesia. *Earth Sciences Malaysia (ESMY)*, *7*(*2*), 75-82. https://doi.org/10.26480/esmy.02.2023.75.82

Simandjuntak, T., Surono, & Sukido. (1993). *Peta Geologi Lembar Kolaka Skala 1:250.*000. Bandung: Pusat Penelitian dan Pengembangan Geologi.

Suryadi, Haerudin, N., Karyanto, & Sudrajat, Y. (2017). Identifikasi Struktur Bawah Permukaan Lapangan Panas Bumi Way Ratai Berdasarkan Data Audio Magnetotelluric (AMT). *Jurnal Geofisika Eksplorasi*, *3*(*1*), 1-12. http://dx.doi.org/10.23960/jge.v3i1.1033

Telford, M, W., L, P, Geldard, R, E, Sheriff, and D, A, Keys, (1990)*, Applied Geophysics 2nd ed*. London: Cambridge University Press.

Tamburaka, E. (2019). Resiko dan Mitigasi Bencana Gempa Tektonik di Kabupaten Konawe. *Jurnal Aksara Publik*, 3(2), 222-235.

Widodo, M., Yulianto, T., Harmoko, U., Yulianto, G., Widada, S., & Dewantoro, Y. (2016). Analisis Struktur Bawah Permukaan Daerah Harjosari Kabupaten Semarang Menggunakan Metode Geomagnet dengan Pemodelan 2D dan 3D. *Youngster Physics Journal*, 5(4), 251-260. https://ejournal3.undip.ac.id/index.php/bfd/article/view/14086

Zakaria Z., & Sidarto. (2015). Aktifitas Tektonik di Sulawesi dan Sekitarnya Sejak Mesozoikum Hingga Kini Sebagai Akibat Interaksi Aktifitas Tektonik Lempeng Tektonik Utama di Sekitarnya. *Jurnal Geologi dan Sumberdaya Mineral*, 16(3), 115-127. https://doi.org/10.33332/jgsm.geologi.v16i3.36